

# The Theoretical Study of $p\bar{p} \rightarrow \bar{\Lambda}\Sigma\eta$ Reaction

Aojia Xu,<sup>1</sup> Ruitian Li,<sup>1</sup> Xuan Luo,<sup>2</sup> and Hao Sun<sup>1,\*</sup>

<sup>1</sup>*School of Physics, Dalian University of Technology, Dalian 116024, People's Republic of China*

<sup>2</sup>*School of Physics and Optoelectronics Engineering, Anhui University, Hefei 230601, People's Republic of China*  
(Dated: April 29, 2024)

We study the production of hyperon resonances in the  $p\bar{p} \rightarrow \bar{\Lambda}\Sigma\eta$  reaction within an effective Lagrangian approach. The model includes the production of  $\Sigma(1750)$  and  $\Lambda(1670)$  in the intermediate state excited by the  $K$  and  $K^*$  meson exchanges between the initial proton and antiproton. Due to the large coupling of  $\Sigma(1750)\Sigma\eta$  vertex,  $\Sigma(1750)$  is found a significant contribution near the threshold in this reaction. We provide total and differential cross section predictions for the reaction and discuss the possible influence of  $\Sigma(1750)\Sigma\eta$  vertex coupling and model parameters, which will be useful in future experimental studies. This reaction can provide a platform for studying the features of  $\Sigma(1750)$  resonance, especially the coupling to  $\Sigma\eta$  channel.

## I. INTRODUCTION

The investigation of the meson-baryon interactions at low energies plays an important role in exploring the features of hyperon resonances. However, experiments on hyperon resonances are not as extensive as those on nucleon resonances. Most of our current knowledge about  $\Sigma$  hyperon resonances has come from the analysis of experimental data in the  $\Lambda\pi$  and  $\bar{K}N$  channels [1–9]. In addition to  $\bar{K}N$  scattering reactions, others such as LEPS [10–12], CLAS [13, 14], COSY [15, 16] have attempted to further generate excited hyperon resonances from  $\gamma N$  and  $NN$  collisions.

Because of the isospin conservation, the  $\Sigma\eta$  channel has a special significance for which it is a pure  $I = 1$  channel that only coupled to  $\Sigma$  hyperon resonances. However, even with this advantage, the researches on  $\Sigma$  hyperon resonances are still relatively few. Up to now, only one  $\Sigma$  hyperon resonance,  $\Sigma(1750)$ , was found to be well coupled to the  $\Sigma\eta$  channel in the Particle Data Group (PDG) [17] book. While the decay branching ratios of other  $\Sigma$  hyperon resonances to this channel are still not well identified, it is possible that other resonances do have rather weak coupling to the  $\Sigma\eta$  channel, thus making it difficult to study their coupling to  $\Sigma\eta$ . It is also the large coupling that makes it possible to distinguish  $\Sigma(1750)$  from other  $\Sigma$  hyperon resonances in  $\Sigma\eta$  channel. Moreover, the threshold energy of  $\Sigma\eta$  channel is about 1.74 GeV, which is very close to the mass of  $\Sigma(1750)$ , providing a suitable place to investigate the features of  $\Sigma(1750)$  resonance.

Nevertheless, the coupling of  $\Sigma(1750)$  and  $\Sigma\eta$  has rarely been studied in previous researches. In the current particle collision experiments, the coupling of  $\Sigma(1750)$  and  $\Sigma\eta$  channel has only been found in  $K^-p \rightarrow \Sigma^0\eta$  reactions [18]. A chiral  $\bar{K}N$  interaction model was used in Refs. [19, 20] to fit the experimental data of the production cross section and analyze the possible resonances in

the reaction process. Ref. [21] used an effective chiral Lagrangian method to study  $\eta$ -baryon interactions at low energies in the  $\eta B \rightarrow \eta B$  process, including the coupling of  $\Sigma(1750)$  and  $\Sigma\eta$ . Some works have investigated the partial wave analysis of  $\bar{K}N$  scattering, such as Ref. [22] using a global multichannel fit for all the  $\bar{K}N$  scattering reactions; Refs. [23, 24] used a dynamic coupled channel model to establish the spectrum of  $\Sigma$  hyperon resonances and extract the resonance parameters, however, the  $\bar{K}N \rightarrow \Sigma\eta$  reaction was not taken into account. Since there are few experiments and researches on  $\Sigma(1750)$  resonance at present, we hope that the reaction we proposed will be helpful to search for  $\Sigma(1750)$  resonance in future experiments.

In the present work, we propose the  $p\bar{p} \rightarrow \bar{\Lambda}\Sigma\eta$  reaction that can be used to investigate the features of  $\Sigma(1750)$  resonance. We investigate the reaction by using an effective Lagrangian approach, focusing on the production of  $\Sigma(1750)$  hyperon resonance. The approach of effective Lagrangian calculating the reaction cross section is widely used to investigate the process of particle collisions for exploring the reaction mechanism between initial and final particles [25–34]. Near the threshold of  $\Sigma\eta$  channel, only  $\Sigma(1750)$  was found to have a relatively large decay branch ratio to  $\Sigma\eta$  channel, which can be naturally regarded that  $\Sigma(1750)$  has a large coupling to  $\Sigma\eta$  channel. Besides, the resonance contribution in the  $\Lambda\eta$  channel should also be taken into account. Same as  $\Sigma(1750)$ , here we only need to consider the contribution of  $\Lambda(1670)$ . In our model, the  $\Sigma(1750)$  and  $\Lambda(1670)$  resonances are excited by the  $K$  and  $K^*$  meson exchanges between the initial proton and antiproton. Other meson exchanges are forbidden by the law of isospin conservation. The predictions of the total cross section and angular distribution, as well as invariant mass distribution are presented in our work, which will be helpful for future comparison with the experimental data. We also provide a discussion for the dependence of total and differential cross sections on model parameters.

Our work is organized as follows. In Sec. II, we introduce the formalism and ingredients necessary of each amplitude in our model and obtain the concrete form of

\* haosun@dlut.edu.cn

amplitudes. The numerical results of the total and differential cross sections for  $p\bar{p} \rightarrow \bar{\Lambda}\Sigma\eta$  reaction are presented in Sec. III. Finally, a short conclusion is made in Sec. IV.

## II. FORMALISM

Within our approach, the production mechanism of the  $\Sigma(1750)$  and  $\Lambda(1670)$  resonances in the reaction  $p\bar{p} \rightarrow \bar{\Lambda}\Sigma\eta$  consists of the standard  $t$ - and  $u$ -channel as shown in Fig. 1. In view of  $\Sigma(1750)$  has a relatively large coupling to the  $\Sigma\eta$  channel, we expect it may give a significant contribution in the reaction. Because of charge, the  $K$  and  $K^*$  exchanges are present only for the charged  $K^+$  and  $K^{*+}$ .

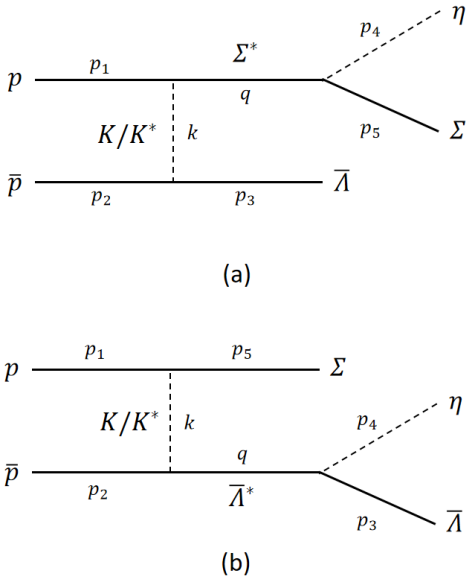


FIG. 1: (a)  $u$ - (b)  $t$ -channel exchanges Feynman diagrams for  $p\bar{p} \rightarrow \bar{\Lambda}\Sigma\eta$  reaction.

The production amplitude is calculated from the following effective Lagrangians,

$$\begin{aligned}
\mathcal{L}_{\Lambda KN} &= -\frac{g_{\Lambda KN}}{m_{\Lambda} + m_N} \bar{\Lambda} \gamma_5 \not{\partial} K N + h.c., \\
\mathcal{L}_{\Sigma^* KN} &= \sqrt{2} i g_{\Sigma^* KN} \bar{\Sigma}^* K N + h.c., \\
\mathcal{L}_{\Sigma\eta\Sigma^*} &= -i g_{\Sigma\eta\Sigma^*} \bar{\Sigma} \eta \Sigma^* + h.c., \\
\mathcal{L}_{\Sigma KN} &= -\frac{\sqrt{2} g_{\Sigma KN}}{m_{\Sigma} + m_N} \bar{\Sigma} \gamma_5 \not{\partial} K N + h.c., \\
\mathcal{L}_{\Lambda^* KN} &= i g_{\Lambda^* KN} \bar{\Lambda}^* K N + h.c., \\
\mathcal{L}_{\Lambda\eta\Lambda^*} &= -i g_{\Lambda\eta\Lambda^*} \bar{\Lambda} \eta \Lambda^* + h.c.,
\end{aligned} \tag{1}$$

and for  $K^*$  exchange,

$$\begin{aligned}
\mathcal{L}_{\Lambda K^* N} &= -g_{\Lambda K^* N} \bar{\Lambda} \left( \gamma^\mu + \frac{\kappa_{\Lambda K^* N}}{2m_N} (p_{K^*}^\mu - \not{p}_{K^*} \gamma^\mu) \right) K_\mu^* N \\
&\quad + h.c., \\
\mathcal{L}_{\Sigma^* K^* N} &= i g_{\Sigma^* K^* N} \bar{\Sigma}^* \gamma_5 \gamma^\mu K_\mu^* N + h.c., \\
\mathcal{L}_{\Sigma K^* N} &= -g_{\Sigma K^* N} \bar{\Sigma} \left( \gamma^\mu + \frac{\kappa_{\Sigma K^* N}}{2m_N} (p_{K^*}^\mu - \not{p}_{K^*} \gamma^\mu) \right) K_\mu^* N \\
&\quad + h.c., \\
\mathcal{L}_{\Lambda^* K^* N} &= i g_{\Lambda^* K^* N} \bar{\Lambda}^* \gamma_5 \gamma^\mu K_\mu^* N + h.c.,
\end{aligned} \tag{2}$$

where  $\kappa_{\Lambda K^* N} = 2.76$  and  $\kappa_{\Sigma K^* N} = -2.33$  [35] are the anomalous magnetic moments. The coupling constants  $g_{\Lambda KN}$ ,  $g_{\Sigma KN}$ ,  $g_{\Lambda K^* N}$  and  $g_{\Sigma K^* N}$  can be determined by the SU(3) predictions [36], which give the values that  $g_{\Lambda KN} = -13.99 \text{ GeV}^{-1}$ ,  $g_{\Sigma KN} = 2.69 \text{ GeV}^{-1}$ ,  $g_{\Lambda K^* N} = -6.21 \text{ GeV}^{-1}$  and  $g_{\Sigma K^* N} = -4.25 \text{ GeV}^{-1}$ . And we take the value for  $\Lambda^* K^* N$  coupling from Ref. [37]. For  $\Sigma^* K^* N$  coupling, we adopt the same value as  $\Sigma^* K N$ , approximatively. Other constants are determined from the partial decay widths, given in Table 1. It should be noted that we use the average values of the branching ratios listed in PDG [17].

TABLE I. Coupling constants used in this work.

State	Width (MeV)	Decay channel	Branching ratio adopted	$g^2/4\pi$
$\Sigma(1750)$	206	$\Sigma\eta$	0.35	$4.05 \times 10^{-1}$
		$NK$	0.09	$1.66 \times 10^{-2}$
$\Lambda(1670)$	32	$\Lambda\eta$	0.175	$4.77 \times 10^{-2}$
		$NK$	0.25	$0.82 \times 10^{-2}$

Since hadrons are not pointlike particles, it is necessary to consider a form factor at each vertex, which can parameterize the structure of the hadron. Here, we introduce the form factor for intermediate baryons as

$$f_B(q_B^2) = \frac{\Lambda_B^4}{\Lambda_B^4 + (q_B^2 - m_B^2)^2}, \tag{3}$$

with  $q_B$  and  $m_B$  the four-momentum and mass of intermediate hadron, respectively. The cut-off parameter for  $\Lambda^*$  exchange is taken as  $\Lambda_{\Lambda^*} = 1.5 \text{ GeV}$ .

For  $K$  meson and  $K^*$  meson exchange diagrams, we introduce the form factor as

$$f_M(k_M^2) = \left( \frac{\Lambda_M^2 - m_M^2}{\Lambda_M^2 - k_M^2} \right)^n, \tag{4}$$

where  $k_M$  and  $m_M$  denote the four-momentum and mass of exchanged meson, respectively. Here, we take  $\Lambda_K = 1.1 \text{ GeV}$  [34] and  $\Lambda_{K^*} = 1.5 \text{ GeV}$  [38, 39] for the corresponding meson exchange. In the calculation,  $n = 1$  for  $K$  exchange and  $n = 2$  for  $K^*$  exchange [40] are adopted.

The propagators for the exchanged particles are expressed as

$$G_K(k) = \frac{i}{(k^2 - m_K^2)}, \quad (5)$$

for  $K$  meson,

$$G_{K^*}^{\mu\nu}(k) = -i \left( \frac{g^{\mu\nu} - \frac{k^\mu k^\nu}{m_{K^*}^2}}{k^2 - m_{K^*}^2} \right), \quad (6)$$

for  $K^*$  meson, and

$$G^{\frac{1}{2}}(q) = \frac{i(q \pm M_B)}{q^2 - M_B^2 + iM_B\Gamma_B}, \quad (7)$$

for spin-1/2 baryons with '+' and '-' correspond to particle and antiparticle respectively, where  $k$  and  $q$  are the four-momentum;  $M_B$  and  $\Gamma_B$  are the mass and width of intermediate baryons.

With the ingredients presented above, the total scattering amplitudes of  $p\bar{p} \rightarrow \bar{\Lambda}\Sigma\eta$  reaction can be written as

$$\begin{aligned} \mathcal{M}_a^K &= \frac{\sqrt{2}ig_{\Sigma\eta\Sigma^*}g_{\Sigma^*Kp}g_{\Lambda Kp}}{m_\Lambda + m_p} f_{K^*}^2(k_1) f_{\Sigma^*}(q_1) \bar{u}(p_5, s_5) \\ &\quad \times G_{\Sigma^*}(q_1) u(p_1, s_1) G_K(k_1) \bar{v}(p_2, s_2) \gamma_5 \not{k}_1 v(p_3, s_3), \\ \mathcal{M}_b^K &= \frac{\sqrt{2}ig_{\Lambda\eta\Lambda^*}g_{\Lambda^*Kp}g_{\Sigma Kp}}{m_\Sigma + m_p} f_{K^*}^2(k_2) f_{\Lambda^*}(q_2) \bar{v}(p_2, s_2) \\ &\quad \times G_{\Lambda^*}(q_2) v(p_3, s_3) G_K(k_2) \bar{u}(p_5, s_5) \gamma_5 \not{k}_2 u(p_1, s_1), \\ \mathcal{M}_a^{K^*} &= -g_{\Sigma\eta\Sigma^*}g_{\Sigma^*K^*p}g_{\Lambda K^*p} f_{K^*}^2(k_1) f_{\Sigma^*}(q_1) \bar{u}(p_5, s_5) \\ &\quad \times G_{\Sigma^*}(q_1) \gamma_5 \gamma^\mu u(p_1, s_1) G_{K^*\mu\nu}(k_1) \bar{v}(p_2, s_2) \\ &\quad \times \left( \gamma^\nu + \frac{\kappa_{\Lambda K^*p}}{2m_p} (k_1^\nu - \not{k}_1 \gamma^\nu) \right) v(p_3, s_3), \\ \mathcal{M}_b^{K^*} &= -g_{\Lambda\eta\Lambda^*}g_{\Lambda^*K^*p}g_{\Sigma K^*p} f_{K^*}^2(k_2) f_{\Sigma^*}(q_2) \bar{v}(p_2, s_2) \\ &\quad \times \gamma^\mu \gamma_5 G_{\Lambda^*}(q_2) v(p_3, s_3) G_{K^*\mu\nu}(k_2) \bar{u}(p_5, s_5) \\ &\quad \times \left( \gamma^\nu + \frac{\kappa_{\Sigma K^*p}}{2m_p} (k_2^\nu - \not{k}_2 \gamma^\nu) \right) u(p_1, s_1). \end{aligned} \quad (8)$$

The  $p_1, p_2, p_3$  and  $p_5$  represent the four-momentums of the  $p, \bar{p}, \bar{\Lambda}$  and  $\Sigma$  baryon, respectively.  $k_1$  and  $k_2$  correspond to the four-momentum of exchanged meson in Fig. 1(a) and Fig. 1(b), respectively.  $q_1$  and  $q_2$  has the same meaning as  $k_1, k_2$ , but for  $\Sigma(1750)$  and  $\Lambda(1670)$ .

The differential and total cross sections for this reaction can be obtained through

$$\begin{aligned} d\sigma &= \frac{(2\pi)^4}{4\sqrt{(p_1 \cdot p_2)^2 - m_p^4}} \left( \frac{1}{4} \sum |\mathcal{M}|^2 \right) d\Phi_3 \\ &= \frac{1}{(2\pi)^4} \frac{1}{\sqrt{(p_1 \cdot p_2)^2 - m_p^4}} \frac{|\vec{p}_3||\vec{p}_5^*|}{32\sqrt{s}} \left( \frac{1}{4} \sum |\mathcal{M}|^2 \right) \\ &\quad dm_{\Sigma\eta} d\Omega_5^* d\cos\theta_3, \end{aligned} \quad (9)$$

where  $p_1, p_2$  represent the four-momentum of the initial particles  $p, \bar{p}$  at total center-of-mass frame;  $\vec{p}_5^*$  stands for the three-momentum of the  $\Sigma$  baryon in the center-of-mass frame of  $\Sigma\eta$  pair.

### III. RESULTS

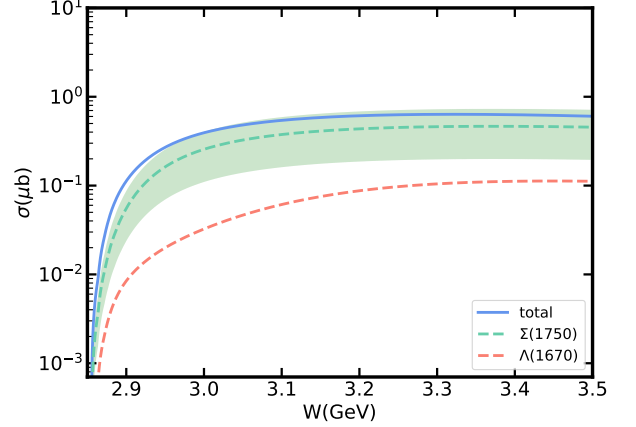


FIG. 2: Total cross section vs center of mass energy  $W$  for  $p\bar{p} \rightarrow \bar{\Lambda}\Sigma\eta$  reaction. The blue curve represents the total cross section including all the contributions in Fig. 1. The green dashed and red dashed curves are the contributions of  $\Sigma(1750)$  and  $\Lambda(1670)$  respectively, with the branching ratio of  $\Sigma^* \rightarrow \Sigma\eta$  takes the middle value 35%. The green band is the branching ratio of  $\Sigma^* \rightarrow \Sigma\eta$  from 15% to 55%.

In this section, we will present the theoretical results of the  $p\bar{p} \rightarrow \bar{\Lambda}\Sigma\eta$  reaction calculated by the model in the previous section, including the total cross section and the differential cross section. Firstly, we consider the effects of the branching ratio  $Br(\Sigma^* \rightarrow \Sigma\eta)$  on the total cross section by fixing the cut-off parameters  $\Lambda_{\Sigma^*} = \Lambda_{\Lambda^*} = 1.5$  GeV. In Fig. 2, we plot the total cross section from the reaction threshold up to 3.5 GeV, together with the individual contributions of  $\Sigma(1750)$  and  $\Lambda(1670)$  resonances. Both contributions of  $K$  and  $K^*$  exchanges are taken into account. It is obvious that  $\Sigma(1750)$  plays a dominant role of this reaction. Even if we take the minimum value of branching ratio that  $Br(\Sigma^* \rightarrow \Sigma\eta) = 15\%$ , the contribution of  $\Sigma(1750)$  is significantly larger than that of  $\Lambda(1670)$  in this reaction. The significant contribution of  $\Sigma(1750)$  is due in part to the coupling of  $\Sigma(1750)\Sigma\eta$  vertex is strong compared to that of  $\Lambda(1670)\Lambda\eta$ . But more importantly, the coupling of  $\Lambda K N$  vertex is more than 5 times that of  $\Sigma K N$  vertex. We extract the coupling constants of the vertex associated with the  $\Sigma(1750)$  from the decay width. However, this approach makes it impossible to determine the relative phase between  $\Sigma(1750)$  and  $\Lambda(1670)$ . Therewith, we consider to detect the existence of interference effects by multiplying a factor of -1 and there is no significant

change in the results. Since  $\Sigma(1750)$  plays a dominant role near the threshold, it can be considered that this reaction provides a good place for studying the nature of  $\Sigma(1750)$  resonance.

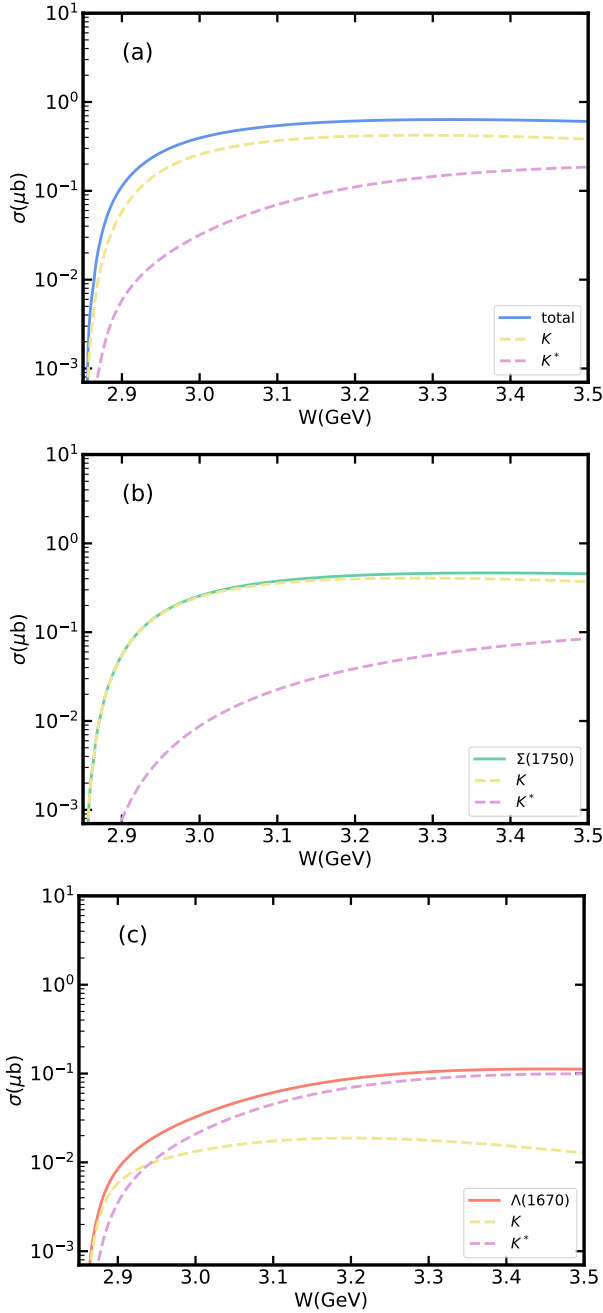


FIG. 3: The cross sections vs center of mass energy  $W$  from  $K^+$  and  $K^{*+}$  exchanges. The blue, green and red curves are the total cross section,  $\Sigma(1750)$  and  $\Lambda(1670)$  contributions, respectively. The yellow dashed and purple dashed represent the  $K^+$  and  $K^{*+}$  mesons exchanged contributions.

Because of the uncertainty of the form factor, it is necessary to consider the effect of form factor on the cross

section. For this reaction, only the effect of form factor on cross sections of  $K^+$  and  $K^{*+}$  exchanges needs to be considered. In Fig. 3, we show the cross sections from  $K^+$  and  $K^{*+}$  exchanges compare to the total cross section and  $\Sigma(1750)$ ,  $\Lambda(1670)$  resonances. The results show clearly that  $K^+$  exchange gives the dominant contribution in total cross section and  $\Sigma(1750)$  contribution. The dominant role of  $K^+$  exchange in  $\Sigma(1750)$  can be attributed to the relatively large  $\Lambda K p$  coupling. While in Fig. 3(c), it shows that  $K^+$  exchange is the main contribution of  $\Lambda(1670)$  near the threshold. With the energy of the center of mass increasing, the contribution of  $K^{*+}$  exchange is becoming more and more significant. Moreover, due to the influence of  $K^{*+}$  exchange, the cross section of  $\Lambda(1670)$  shows a relatively obvious trend of gradual increase.

Next, we consider the dependence of the cross section on the model parameter  $\Lambda_{\Sigma^*}$  introduced by the form factor. In Fig. 4, we present the cross sections of  $K^+$  and  $K^{*+}$  exchanges with three cut-off parameters  $\Lambda_{\Sigma^*} = 1.2, 1.5, 1.8$  GeV. Whether near the threshold or at higher energies, the  $K^+$  exchange is more sensitive to the change of cut-off parameter  $\Lambda_{\Sigma^*}$ . In addition, due to

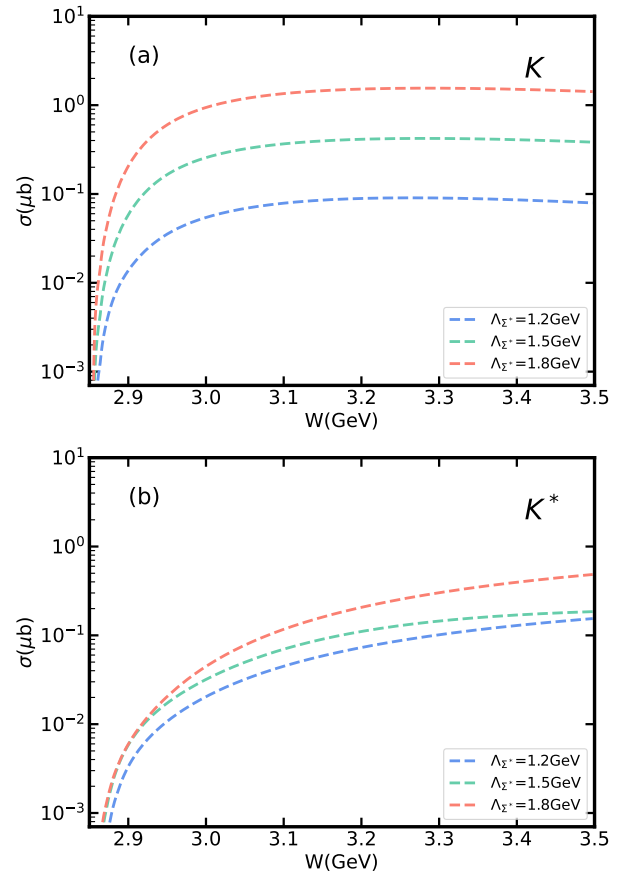


FIG. 4: The cross sections vs center of mass energy  $W$  from the  $K^+$  and  $K^{*+}$  mesons exchanged contributions with the different values of cut-off parameter  $\Lambda_{\Sigma^*}$ .

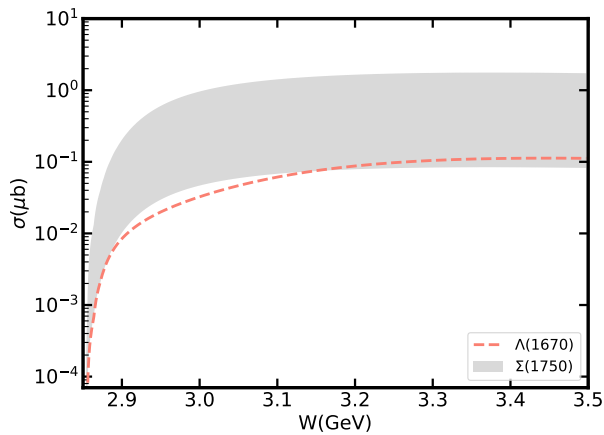


FIG. 5: The cross sections vs center of mass energy  $W$  from the individual contributions of  $\Sigma(1750)$  and  $\Lambda(1670)$ . The band corresponds to the results of  $\Sigma(1750)$  by varying the cut-off parameter  $\Lambda_{\Sigma^*}$  for  $\Sigma(1750)KN$  vertex from 1.2 to 1.8 GeV.

the dominant role of the  $K^+$  exchange in  $\Sigma(1750)$  contribution, the  $\Sigma(1750)$  contribution also has a strong dependence on the value of  $\Lambda_{\Sigma^*}$ , as shown in Fig. 5. When  $\Lambda_{\Sigma^*}$  is larger than 1.2 GeV,  $\Sigma(1750)$  plays a main role in total cross section. If we take  $Br(\Sigma^* \rightarrow \Sigma\eta) = 15\%$ , this value will be raised to 1.4 GeV. At  $\Lambda_{\Sigma^*} = 1.2$  GeV,  $\Sigma(1750)$  dominates at lower energy, and  $\Lambda(1670)$  gradually contributes more than  $\Sigma(1750)$  as the energy increases. When  $\Lambda_{\Sigma^*}$  is below 1.2 GeV, the  $\Lambda(1670)$  becomes the dominant contribution. However, since the cut-off parameter is often regarded as a free parameter, more experimental data are needed to determine it.

In addition to the total cross section, we also study the differential cross section of  $p\bar{p} \rightarrow \bar{\Lambda}\Sigma\eta$  with the center of mass energy  $W = 3.1$  GeV, shown in Fig. 6, where  $\Sigma(1750)$  is the main contribution. As can be seen from Fig. 6(a) and 6(b), there is an obvious peak of  $\Sigma(1750)$

contribution in  $\Sigma\eta$  invariant mass distribution. However, due to the influence of  $\Lambda(1670)$ , the peak energy of the total contribution is slightly higher than that in  $\Sigma(1750)$ . If we adopt  $Br(\Sigma^* \rightarrow \Sigma\eta) = 15\%$ ,  $\Lambda(1670)$  will enhance the total contribution more significantly. The change in the coupling constant due to the decay width makes the total contribution for  $Br(\Sigma^* \rightarrow \Sigma\eta) = 55\%$  about 4 times that for  $Br(\Sigma^* \rightarrow \Sigma\eta) = 15\%$ . In Fig. 6(c), the dominant role of  $\Sigma(1750)$  in the  $u$ -channel is clearly shown as the backward enhancement of the angular distribution of  $\bar{\Lambda}$ . Compared to  $\Sigma(1750)$ , the contribution of  $\Lambda(1670)$  is small in both the  $\bar{\Lambda}$  and  $\eta$  angular distributions, but its forward angle of the  $\eta$  angular distribution significantly affects the shape of the total contribution.

#### IV. CONCLUSION

We have made a theoretical study of  $p\bar{p} \rightarrow \bar{\Lambda}\Sigma\eta$  reaction based on an effective Lagrangian approach. In our model, we consider the production of  $\Sigma(1750)$  and  $\Lambda(1670)$  as intermediate states excited by the  $K$  and  $K^*$  meson exchanges between the initial proton and antiproton. We provide a prediction of total and differential cross sections and discuss the possible influence of  $\Sigma(1750)\Sigma\eta$  vertex coupling and model parameters. According to our results,  $\Sigma(1750)$  resonance makes a significant contribution near the threshold, making the reaction suitable for studying the features of  $\Sigma(1750)$  resonance.

#### V. ACKNOWLEDGMENTS

HS is supported by the National Natural Science Foundation of China (Grant No.12075043). XL is supported by the National Natural Science Foundation of China under Grant No.12205002.

- 
- [1] S. Prakhov et al. Measurement of  $\pi^0$  Lambda, anti-K0 n, and  $\pi^0$  Sigma0 production in K- p interactions for p(K-) between 514 and 750-MeV/c. *Phys. Rev. C*, 80:025204, 2009.
  - [2] W. Cameron, B. Franek, G. P. Gopal, G. E. Kalmus, T. C. Bacon, I. Butterworth, and R. A. Stern. New High Statistics Data on  $K^-p \rightarrow$  Two-body Final States Over the Center-of-mass Energy Range 1720-MeV to 1796-MeV. *Nucl. Phys. B*, 193:21–52, 1981.
  - [3] W. A. Morris, John R. Albright, A. P. Colleraine, J. D. Kimel, and J. E. Lannutti. Reaction K- n  $\rightarrow$  Lambda0 pi- from 1550-MeV to 1650-MeV. *Phys. Rev. D*, 17:55–61, 1978.
  - [4] R. A. Ponte, Stanley S. Hertzbach, Janice Button-Shafer, S. S. Yamamoto, E. L. Hart, R. M. Rice, R. B. Bacastow, and S. Y. Fung. Reaction K- p  $\rightarrow$  Lambda pi0 from 1647-MeV to 1715-MeV. *Phys. Rev. D*, 12:2597–2609, 1975.
  - [5] B. Conforto, G. P. Gopal, G. E. Kalmus, Peter J. Litchfield, R. T. Ross, A. J. Van Horn, T. C. Bacon, I. Butterworth, E. F. Clayton, and R. M. Waters. K- p Reactions from 0.96-GeV/c to 1.355-GeV/c Involving Two-Body Final States. *Nucl. Phys. B*, 105:189–221, 1976.
  - [6] Terry S. Mast, Margaret Alston-Garnjost, Roger O. Bangerter, Angela S. Barbaro-Galtieri, Frank T. Solmitz, and Robert D. Tripp. Elastic, Charge Exchange, and Total K- p Cross-Sections in the Momentum Range 220-MeV/c to 470-MeV/c. *Phys. Rev. D*, 14:13, 1976.
  - [7] M. Jones, R. Levi Setti, D. Merrill, and R. D. Tripp. K- p Charge Exchange and Hyperon Production Cross-Sections from 860-MeV/c to 1000-MeV/c. *Nucl. Phys. B*, 90:349–383, 1975.

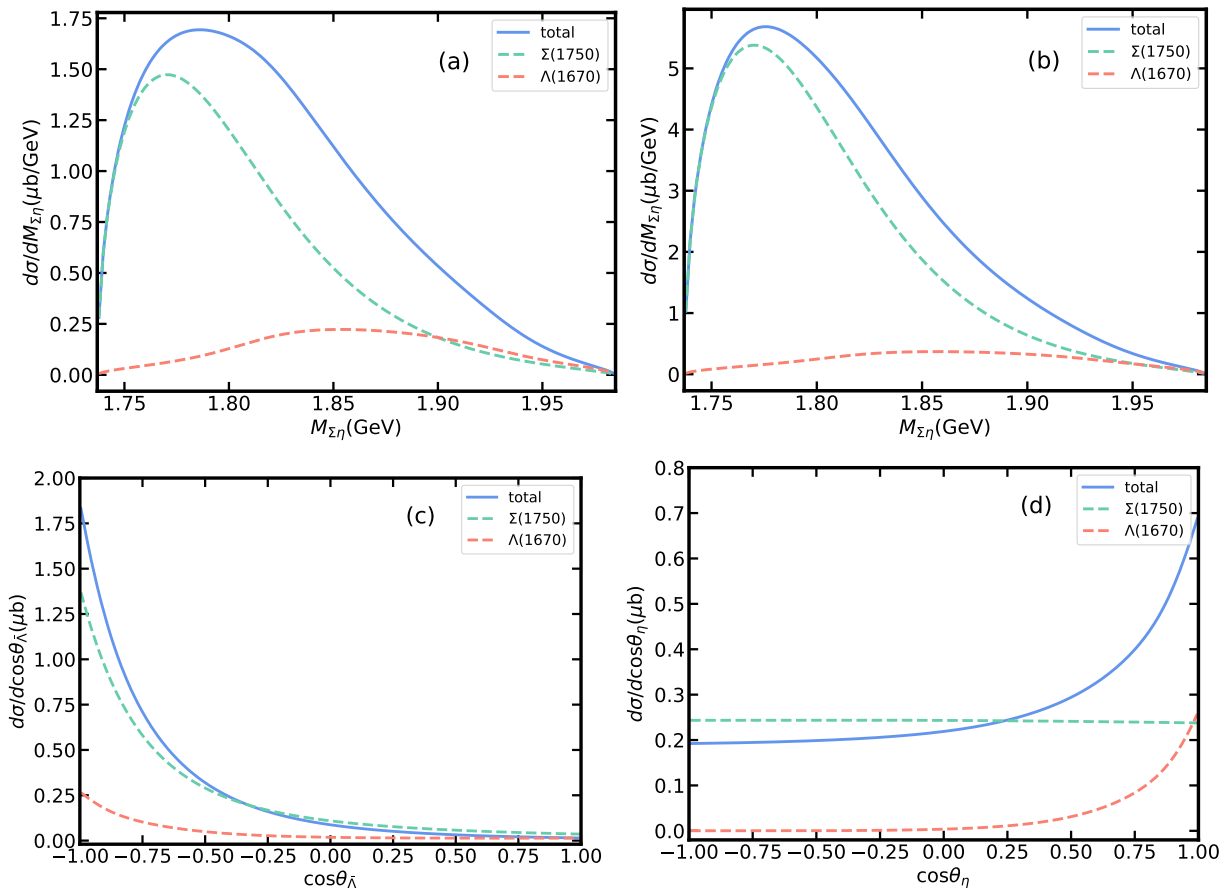


FIG. 6: At center of mass energy  $W = 3.1$  GeV, (a)-(b) invariant mass distribution of final  $\Sigma\eta$  pair for  $p\bar{p} \rightarrow \bar{\Lambda}\Sigma\eta$  reaction with  $Br(\Sigma^* \rightarrow \Sigma\eta) = 15\%$  and  $55\%$ , respectively; (c) the angular distribution of  $\bar{\Lambda}$ ; (d) the angular distribution of  $\eta$  in the  $\Sigma\eta$  rest frame.

- [8] D. F. Baxter et al. A study of neutral final states in k-p interactions in the range from 690 to 934 meV/c. *Nucl. Phys. B*, 67:125–156, 1973.
- [9] R. Armenteros et al. K- p cross-sections from 440 to 800 meV/c. *Nucl. Phys. B*, 21:15–76, 1970.
- [10] S. Y. Ryu et al. Interference effect between  $\phi$  and  $\Lambda(1520)$  production channels in the  $\gamma p \rightarrow K^+ K^- p$  reaction near threshold. *Phys. Rev. Lett.*, 116(23):232001, 2016.
- [11] H. Kohri et al. Near-threshold Lambda(1520) production by the vec-gamma p  $\rightarrow$  K+ Lambda(1520) reaction at forward K+ angles. *Phys. Rev. Lett.*, 104:172001, 2010.
- [12] M. Niiyama et al. Photoproduction of Lambda(1405) and Sigma0(1385) on the proton at  $E(\gamma) = 1.5$ -2.4-GeV. *Phys. Rev. C*, 78:035202, 2008.
- [13] U. Shrestha et al. Differential cross sections for  $\Lambda(1520)$  using photoproduction at CLAS. *Phys. Rev. C*, 103(2):025206, 2021.
- [14] K. Moriya et al. Differential Photoproduction Cross Sections of the  $\Sigma^0(1385)$ ,  $\Lambda(1405)$ , and  $\Lambda(1520)$ . *Phys. Rev. C*, 88:045201, 2013. [Addendum: *Phys.Rev.C* 88, 049902 (2013)].
- [15] Izabella Zychor. Excited Hyperons Produced in Proton-Proton Collisions with Anke at COSY. *Int. J. Mod. Phys. E*, 18:241–247, 2009.
- [16] I. Zychor et al. Evidence for an excited hyperon state in  $pp \rightarrow p K^+ Y_0^*$ . *Phys. Rev. Lett.*, 96:012002, 2006.
- [17] R. L. Workman et al. Review of Particle Physics. *PTEP*, 2022:083C01, 2022.
- [18] M. D. Jones. A study of the reaction k- p  $\rightarrow$  sigma0 eta near threshold. *Nucl. Phys. B*, 73:141–165, 1974.
- [19] Albert Feijoo, Daniel Gazda, Volodymyr Magas, and Àngels Ramos.  $\bar{K}N$  interaction, p-wave terms. *EPJ Web Conf.*, 271:07002, 2022.
- [20] Albert Feijoo, Daniel Gazda, Volodymyr Magas, and Àngels Ramos. The  $K^-N$  Interaction in Higher Partial Waves. *Symmetry*, 13(8):1434, 2021.
- [21] Marcelo G. L. Nogueira-Santos and C. C. Barros, Jr. Low energy eta-baryon interaction. *Nucl. Phys. A*, 1039:122740, 2023.
- [22] H. Zhang, J. Tulpan, M. Shrestha, and D. M. Manley. Multichannel parametrization of  $\bar{K}N$  scattering amplitudes and extraction of resonance parameters. *Phys. Rev. C*, 88(3):035205, 2013.
- [23] H. Kamano, S. X. Nakamura, T. S. H. Lee, and T. Sato. Dynamical coupled-channels model of  $K^-p$  reactions. II. Extraction of  $\Lambda^*$  and  $\Sigma^*$  hyperon resonances. *Phys. Rev. C*, 92(2):025205, 2015. [Erratum: *Phys.Rev.C* 95, 049903 (2017)].

- [24] H. Kamano, S. X. Nakamura, T. S. H. Lee, and T. Sato. Dynamical coupled-channels model of  $K^-p$  reactions: Determination of partial-wave amplitudes. *Phys. Rev. C*, 90(6):065204, 2014.
- [25] Jun Shi, Long-Cheng Gui, Jian Liang, and Guoming Liu.  $\Sigma$  Resonances from a Neural Network-based Partial Wave Analysis on  $K^-p$  Scattering. 5 2023.
- [26] Sang-Ho Kim, K. P. Khemchandani, A. Martinez Torres, Seung-il Nam, and Atsushi Hosaka. Photoproduction of  $\Lambda^*$  and  $\Sigma^*$  resonances with  $J^P = 1/2^-$  off the proton. *Phys. Rev. D*, 103(11):114017, 2021.
- [27] Bo-Chao Liu and Ke Wang. Studying  $\Lambda^*$  resonances in the  $p\bar{p} \rightarrow \Lambda\bar{\Lambda}\eta$  reaction. *Phys. Rev. D*, 101(11):114030, 2020.
- [28] Jun-Zhang Wang, Hao Xu, Ju-Jun Xie, and Xiang Liu. Production of the charmoniumlike state  $Y(4220)$  through the  $p\bar{p} \rightarrow Y(4220)\pi^0$  reaction. *Phys. Rev. D*, 96(9):094004, 2017.
- [29] Ju-Jun Xie, Jia-Jun Wu, and Bing-Song Zou. Role of the possible  $\Sigma^*(\frac{1}{2}^-)$  state in the  $\Lambda p \rightarrow \Lambda p\pi^0$  reaction. *Phys. Rev. C*, 90(5):055204, 2014.
- [30] Puze Gao, Jun Shi, and B. S. Zou. Study of  $\Sigma^*$  Resonances from  $K^-N \rightarrow \pi\Lambda$  Reactions. *Few Body Syst.*, 54(7-10):1161–1165, 2013.
- [31] Puze Gao, Jun Shi, and B. S. Zou.  $\Sigma$  Resonances from  $K^-N \rightarrow \pi\Lambda$  reactions with the center of mass energy from 1550 to 1676 MeV. *Phys. Rev. C*, 86:025201, 2012.
- [32] D. A. Sharov, V. L. Korotkikh, and D. E. Lanskoj. Phenomenological model for the  $K\bar{p} N \rightarrow K \Xi$  reaction. *Eur. Phys. J. A*, 47:109, 2011.
- [33] J. Ka Shing Man, Yongseok Oh, and K. Nakayama. Role of high-spin hyperon resonances in the reaction of  $\gamma p \rightarrow K^+K^+\Xi^-$ . *Phys. Rev. C*, 83:055201, 2011.
- [34] Yongseok Oh and Hungchong Kim.  $K^*$  photoproduction off the nucleon:  $\gamma N \rightarrow K^* \Lambda$ . *Phys. Rev. C*, 73:065202, 2006.
- [35] A. C. Wang, W. L. Wang, F. Huang, H. Haberzettl, and K. Nakayama. Nucleon resonances in  $\gamma p \rightarrow K^{*+}\Lambda$ . *Phys. Rev. C*, 96:035206, 2017.
- [36] D. Ronchen, M. Doring, F. Huang, H. Haberzettl, J. Haidenbauer, C. Hanhart, S. Krewald, U. G. Meissner, and K. Nakayama. Coupled-channel dynamics in the reactions  $\pi N \rightarrow \pi N, \eta N, K\Lambda, K\Sigma$ . *Eur. Phys. J. A*, 49:44, 2013.
- [37] Li-Ye Xiao, Qi-Fang Lü, Ju-Jun Xie, and Xian-Hui Zhong. Role of  $\Lambda(1670)$  in the  $\gamma p \rightarrow K^+\eta\Lambda$  reaction near threshold. *Eur. Phys. J. A*, 51(10):130, 2015.
- [38] Bo-Chao Liu and Ju-Jun Xie.  $K^-p \rightarrow \eta\Lambda$  reaction in an effective Lagrangian model. *Phys. Rev. C*, 85:038201, 2012.
- [39] Bo-Chao Liu and Ju-Jun Xie. Evidence for a narrow  $D_{03}$  state in  $K^-p \rightarrow \eta\Lambda$  near threshold. *Phys. Rev. C*, 86:055202, 2012.
- [40] F. Huang, H. Haberzettl, and K. Nakayama. Combined analysis of  $\eta'$  production reactions:  $\gamma N \rightarrow \eta'N, NN \rightarrow NN\eta'$ , and  $\pi N \rightarrow \eta'N$ . *Phys. Rev. C*, 87:054004, 2013.